Current Biology 16, 2035–2041, October 24, 2006 ©2006 Elsevier Ltd All rights reserved DOI 10.1016/j.cub.2006.08.093

Report

Cap-Dependent Translational Inhibition Establishes Two Opposing Morphogen Gradients in *Drosophila* Embryos

Park F. Cho,[1] Chiara Gamberi,[2] Yoon Andrew Cho-Park,[1,3,4] Ian B. Cho-Park,[1,3] Paul Lasko,[2,*] and Nahum Sonenberg[1,*]

[1] Department of Biochemistry and McGill Cancer Center
McGill University
3655 Promenade Sir William Osler
Montréal, Québec H3G 1Y6
Canada

[2] Department of Biology
McGill University
1205 Avenue Dr. Penfield
Montréal, Québec H3A 1B1
Canada

Summary

In the early *Drosophila* embryo, asymmetric distribution of transcription factors, established as a consequence of translational control of their maternally derived mRNAs, initiates pattern formation [1–4]. For instance, translation of the uniformly distributed maternal *hunchback* (*hb*) mRNA is inhibited at the posterior to form an anterior-to-posterior protein concentration gradient along the longitudinal axis [5, 6]. Inhibition of *hb* mRNA translation requires an mRNP complex (the NRE complex), which consists of Nanos (Nos), Pumilio (Pum), and Brain tumor (Brat) proteins, and the Nos responsive element (NRE) present in the 3′ UTR of *hb* mRNA [7–9]. The identity of the mRNA 5′ effector protein that is responsible for this translational inhibition remained elusive. Here we show that d4EHP, a cap binding protein that represses *caudal* (*cad*) mRNA translation [10], also inhibits *hb* mRNA translation by interacting simultaneously with the mRNA 5′ cap structure (m^7GpppN, where N is any nucleotide) [11] and Brat. Thus, by regulating Cad and Hb expression, d4EHP plays a key role in establishing anterior-posterior axis polarity in the *Drosophila* embryo.

Results and Discussion

Transcription is globally repressed in the rapidly dividing nuclei of early *Drosophila* embryos, and therefore gene expression is largely regulated by translational control of maternally provided mRNAs [1]. Translation is often regulated at initiation, which occurs in multiple steps starting with the recruitment of the 40S ribosomal subunit to the 5′ end of an mRNA and resulting in the correct positioning of the 80S ribosome at the initiation codon [12, 13]. Recognition of the cap structure by eIF4F (composed of three subunits, eIF4E, eIF4A, and eIF4G) is an integral part of this process. Moreover, eIF4G interacts both with eIF4E and the poly(A) binding protein (PABP), thus circularizing the mRNA, which in turn is believed to promote reinitiation [2, 14, 15]. Consistent with their importance, eIF4E and PABP have emerged as major targets of translational regulatory mechanisms mediated by such modulator proteins as 4E-BPs and Paip2 [15–17].

Embryonic development in many metazoans requires the activity of various maternal determinants called morphogens, whose spatial and temporal expression is tightly regulated [1–4]. In *Drosophila*, local morphogen concentrations are important for the establishment of polarity and subsequent organization of both the anteroposterior and dorsoventral axes of the embryo. A key morphogen for anteroposterior patterning is the transcription factor Hunchback (Hb); when maternal Hb is allowed to accumulate inappropriately, posterior segmentation is blocked [8, 18, 19]. Two modes of translational control have been proposed for the establishment of the maternal Hb gradient: translational silencing via deadenylation [20] and inhibition at the initiation step in a cap-dependent manner [9].

d4EHP, an eIF4E-like cap binding protein that does not interact with deIF4G and d4E-BP, inhibits the translation of *cad* mRNA by interacting simultaneously with the cap and Bicoid (Bcd) [10]. While many embryos (~41%) produced by females homozygous for the $d4EHP^{CP53}$ mutation showed anterior patterning defects consistent with mislocalized Cad, some (~7%) also exhibited patterning defects such as missing abdominal segments [10] that cannot be readily explained by ectopic Cad expression. Since inhibition of *hb* mRNA translation has been linked in one study to the cap structure [9], and since these additional phenotypes could be consistent with inappropriate regulation of Hb, we investigated the role of d4EHP in Hb expression. Embryos (0–2 hr) from females homozygous for the $d4EHP^{CP53}$ mutation [10] were collected and immunostained with Hb antibody. DNA was stained with DAPI to highlight the nuclei (Figures 1A–1E). For simplicity, embryos will subsequently be referred to by their maternal genotype. To evaluate the extent of the Hb gradient, we measured its signal intensity at 38–50 locations along the anterior-posterior axes of 6–16 embryos of each genotype. We corrected the values for overall signal intensity and then normalized the data for embryo length (EL, anterior pole = 0%, posterior pole = 100%, see Experimental Procedures). The normalized values were plotted and average intensity values were calculated to obtain an average trend (see Experimental Procedures; Figures 1F and 1G). We observed that in Ore^R embryos, Hb signal intensity drops steeply in the middle of the embryo (Figure 1A) and reaches 50% maximum intensity at 48% EL (Figure 1F). In $d4EHP^{CP53}$ embryos, the Hb expression domain extended substantially farther toward the posterior (Figure 1B) and signal intensity remained at approximately 50% of the maximum throughout the

*Correspondence: paul.lasko@mcgill.ca (P.L.), nahum.sonenberg@mcgill.ca (N.S.)
[3] These authors contributed equally to this work.
[4] Present address: Department of Medicine, Massachusetts General Hospital, Harvard Medical School, Boston, Massachusetts 02114.

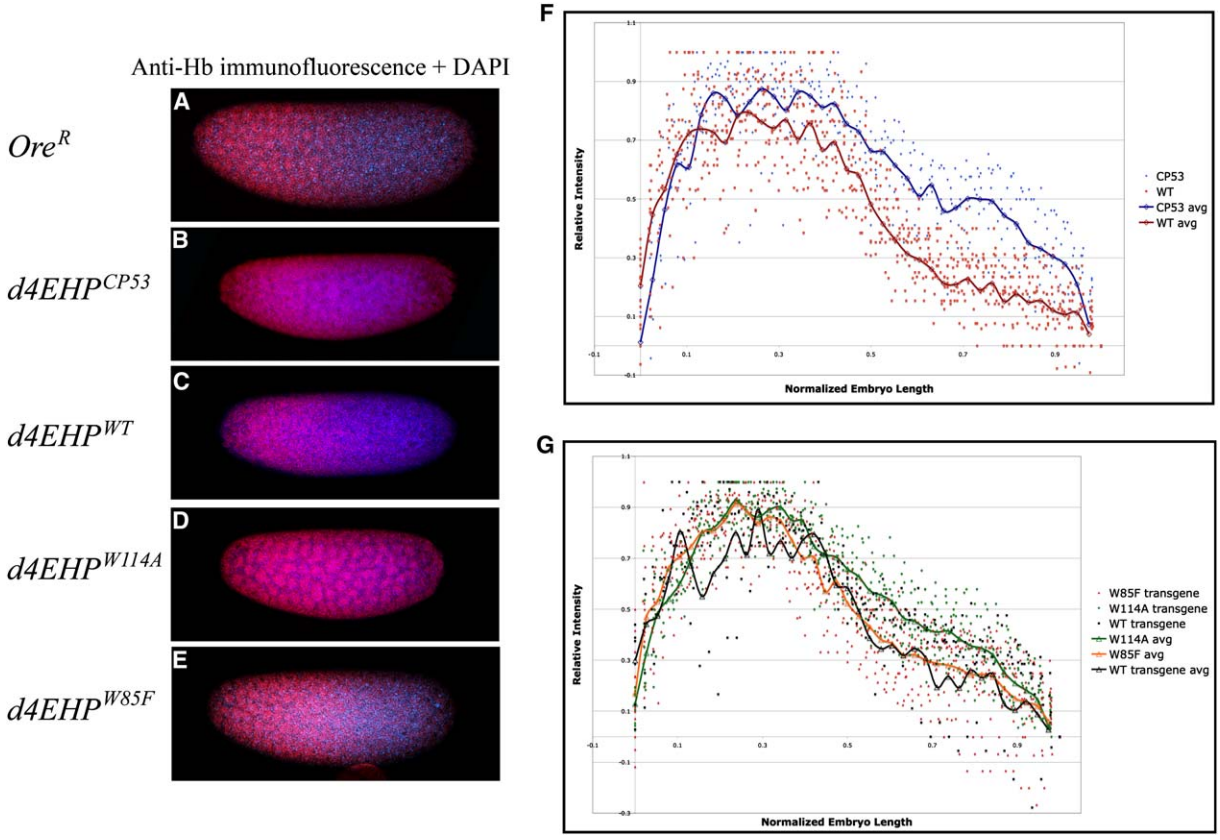

Figure 1. d4EHP Interaction with the Cap Structure Is Required for *hb* Translation Inhibition

Hb immunostaining appears red, and DAPI (blue) was used to stain nuclei.

(A–E) Confocal images are focused on the embryo surface to illustrate the Hb gradient, and therefore not all nuclei are in focus.

(A) Ore^R embryos display normal Hb gradient.

(B) $d4EHP^{CP53}$ mutant embryos show extended Hb expression into the posterior half.

(C) Expression of $d4EHP^{WT}$ transgene in the $d4EHP^{CP53}$ mutant background rescues the mutant phenotype.

(D) Embryos derived from females expressing $d4EHP^{W114A}$ fail to fully repress posterior Hb expression.

(E) Embryos derived from females expressing $d4EHP^{W85F}$ show wild-type Hb distribution pattern.

(F) Plot of normalized Hb intensities measured from wt (red) and $d4EHP^{CP53}$ (blue) embryos. Calculated average intensity values were used to generate average trends (thick lines). The low-intensity values at the anterior pole (near 0% EL) derive from focal deformation of the image (the focus was on the embryo surface).

(G) Plot of normalized Hb intensities measured from $d4EHP^{CP53}$ embryos rescued with different *d4EHP* transgenes ($d4EHP^{wt}$ black, $d4EHP^{W114A}$ green, $d4EHP^{W85F}$ orange). The average trends were calculated as in (F). The posterior pole is indicated as 100% (A–E) or 1 (F, G). Orientation of embryos is anterior left and dorsal up.

region between 50% and 75% EL (Figure 1F). Normal Hb distribution was restored to $d4EHP^{CP53}$ mutant embryos by transgene-derived expression of wild-type *d4EHP* ($d4EHP^{wt}$, Figures 1C and 1G), but not by expression of a mutant form of *d4EHP* ($d4EHP^{W114A}$), which is unable to bind the cap structure (Figures 1D and 1G). Expression of another form of *d4EHP* ($d4EHP^{W85F}$), which cannot bind Bcd, fully rescued the defective Hb gradient (Figures 1E and 1G). The expression levels of the wild-type and mutant *d4EHP* transgenes are essentially equal [10]. Distributions of Nos, Pum, and Brat were unaffected in $d4EHP^{CP53}$ mutant embryos (Figure S1 in the Supplemental Data available online). Taken together, these data demonstrate that d4EHP plays a key role in establishing the posterior boundary of Hb expression in a manner that requires its cap binding activity but not an association with Bcd.

We reasoned that Brat might be a candidate partner protein for d4EHP, since both are relevant for *hb* regulation. Thus, we investigated whether d4EHP and Brat physically interact in vivo. Extracts prepared from 0 to 2 hr Oregon-R (Ore^R) embryos were treated with RNase and used to examine the interaction between Brat and d4EHP. Western blotting analysis with antibodies against d4EHP [10] and Brat (Figure S2) demonstrates that, while anti-d4EHP coimmunoprecipitated endogenous Brat (Figure 2A; lane 3), preimmune serum did not (lane 2). To further demonstrate the specificity of this interaction, HA-tagged deIF4EI and the RNA-binding protein La (negative controls) were transfected in HEK293 cells along with FLAG-tagged full-length Brat. While FLAG antibody immunoprecipitated wild-type HA-d4EHP together with FLAG-Brat (Figure 2B, lane 2), deIF4EI and La failed to coimmunoprecipitate (lanes 1 and 3). Similarly, other RNA-binding proteins such as hnRNP U and HuR, and a d4EHP mutant (W173A), in which a tryptophan residue that is part of the hydrophobic core and thus affects protein folding is replaced,

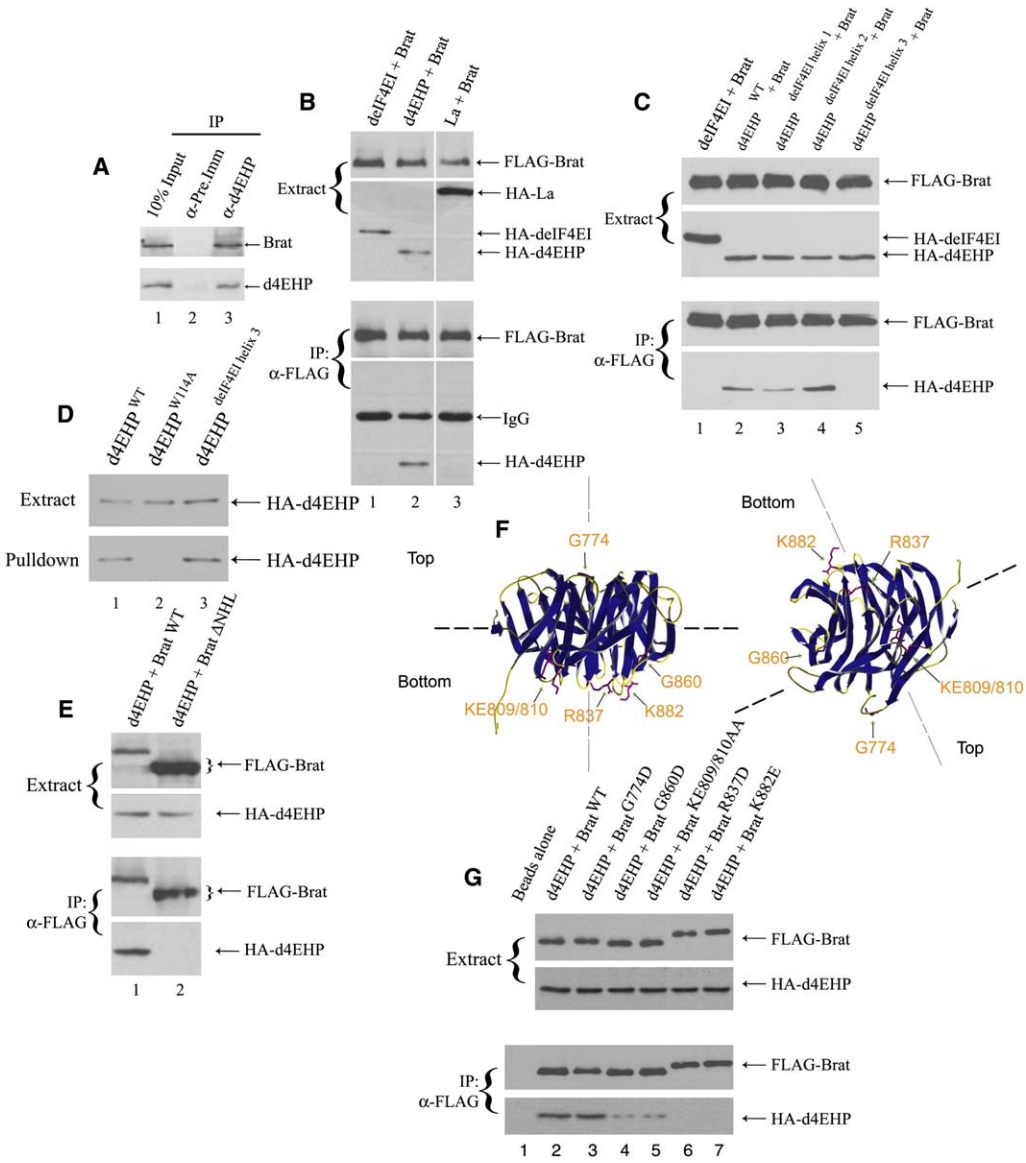

Figure 2. Characterization of the d4EHP:Brat Interaction

(A) d4EHP interacts with Brat in vivo. *Ore*^{R} embryo (0–2 hr) extract (lane 1) was immunoprecipitated with preimmune (lane 2) or anti-d4EHP (lane 3) antisera. Eluted proteins were analyzed by western blotting for the presence of Brat (top) and d4EHP (bottom).

(B) d4EHP interacts specifically with Brat. FLAG-tagged Brat was transfected in HEK293 cells together with HA-tagged deIF4EI, d4EHP, or La. Proteins from cell extracts were immunoprecipitated (IP) with an FLAG antibody and analyzed by western blotting with antibodies against FLAG and HA.

(C) The d4EHP:Brat interaction is mediated by the third dorsal α helix of d4EHP. FLAG-tagged Brat wild-type NHL domain was transfected in HEK293 cells together with HA-tagged deIF4EI, d4EHP, or d4EHP/deIF4EI chimeras.

(B and C) Proteins from cell extracts were immunoprecipitated (IP) with a FLAG antibody and analyzed by western blotting with antibodies against FLAG and HA.

(D) The d4EHP$^{\text{deIF4EI helix 3}}$ mutant interacts with the cap. HEK293 cell extracts (top) containing transfected HA-tagged wild-type d4EHP (lane 1), d4EHP^{W114A} (lane 2), and d4EHP$^{\text{deIF4EI helix 3}}$ (lane 3) were incubated with m^{7}GTP-Sepharose, and the eluate was analyzed by western blotting (bottom).

(E) d4EHP interacts with the Brat C-terminal NHL domain. FLAG-tagged Brat wild-type or ΔNHL mutant were transfected in HEK293 cells with HA-tagged d4EHP, and cell extracts were subjected to western blotting (top). Cell extracts were immunoprecipitated with a FLAG antibody and analyzed by western blotting (bottom).

(F) Ribbon diagrams of the Brat NHL domain [21]. The positions of select surface residues are indicated.

(G) Interaction of Brat mutants with d4EHP. FLAG-tagged wild-type (lane 2) or mutants of the Brat NHL domain (lanes 3–7) were transfected in HEK293 cells together with HA-tagged d4EHP, and cell extracts were subjected to western blotting (top). Cell extracts were immunoprecipitated with a FLAG antibody and eluted proteins were analyzed for the presence of FLAG-Brat and HA-d4EHP by western blotting (bottom). All proteins shown migrated at the positions expected from their molecular mass, as compared with molecular weight markers run on the same gels (data not shown).

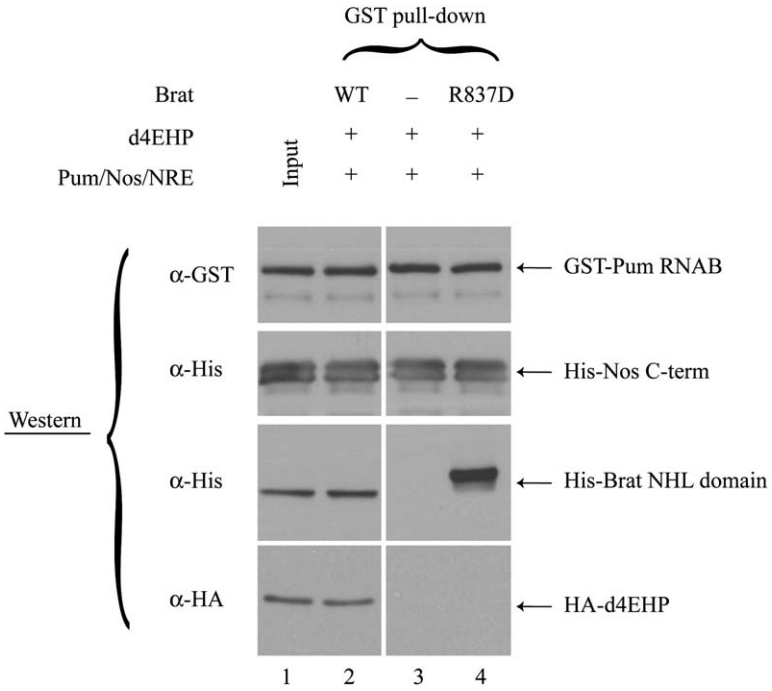

Figure 3. d4EHP Interacts with the NRE Complex In Vitro

Samples containing in vitro translated HA-tagged d4EHP and purified components of the NRE complex were used to perform an in vitro GST pull-down experiment. Eluted proteins were analyzed for the presence of GST-Pum RNAB, His_6-Nos C-term, His_6-Brat NHL domain, and HA-d4EHP by western blotting. All proteins shown migrated at the positions expected from their molecular mass, as compared with molecular weight markers run on the same gels (data not shown).

also failed to interact with Brat (data not shown), demonstrating that Brat interacts specifically with d4EHP. Since we used a cell transfection system to assay for the d4EHP:Brat interaction, it is possible that other bridging proteins are required for the d4EHP-Brat association.

To identify the Brat-interacting domain of d4EHP, we first mutated a number of individual residues located on its convex dorsal surface and tested for coimmunoprecipitation with Brat. From this work, we were unable to identify a point mutant of d4EHP that abrogated the interaction (data not shown). As an alternative approach, we created chimeric proteins in which different domains of d4EHP were replaced with their counterparts from deIF4EI, taking advantage of our knowledge that, unlike d4EHP, deIF4EI does not interact with Brat (Figure 2C, lane 1). We produced three mutant forms of d4EHP, with each one of its three dorsal α helices [21] replaced with that of deIF4EI. We found that while helix 1 and 2 mutants failed to disrupt binding to Brat (Figure 2C, lanes 3 and 4), replacement of d4EHP helix 3 (residues 179–194) significantly reduced the interaction with Brat (Figure 2C, lane 5). Consistent with these observations, α helix 3 is the most divergent between d4EHP and deIF4EI [10]. The overall structure of d4EHP is not affected by the replacement of helix 3 with its deIF4EI counterpart, since the chimeric protein still binds to the cap (Figure 2D, lane 3). Thus, our data demonstrate that Brat interacts with d4EHP on its convex dorsal surface and that this interaction is mediated by the third α helix of d4EHP.

A C-terminal domain of Brat termed the NHL domain is both necessary and sufficient to inhibit *hb* mRNA translation [7]. The NHL domain contains two large surfaces (defined as top and bottom) that can support protein-protein interactions [22]. While the top surface of the NHL domain binds to Pum and Nos, the bottom surface does not interact with any known protein [7, 22]. Although the Brat NHL domain contains an amino acid sequence that conforms to the YxxxxxxLΦ d4EHP binding motif [10], the d4EHP:Brat interaction does not require this motif, since a Brat deletion mutant that lacks it can still interact with both d4EHP and the d4EHP W85F mutant (Figure S3). This sequence is most probably masked from interaction with d4EHP because it is located in the hydrophobic core of the NHL domain [22]. To determine whether the d4EHP:Brat interaction requires the NHL domain, a Brat mutant that lacks the domain (Brat ΔNHL) was engineered and used in a coimmunoprecipitation experiment (Figure 2E). While wild-type Brat was readily coimmunoprecipitated with d4EHP, the Brat ΔNHL mutant was not (compare lanes 1 and 2). Thus, we conclude that the NHL domain is the site of d4EHP interaction. To further characterize this interaction, point mutations were designed to replace residues on the two surfaces of the NHL domain (Figure 2F), and the mutant proteins were tested for their ability to interact with d4EHP. Mutation of a top surface residue that affects Brat interaction with Pum (G774A; Figure 2G, lane 3) [7] did not affect the d4EHP:Brat interaction. However, when residues on the bottom surface were mutated, the d4EHP:Brat interaction was either significantly reduced (G860D and KE809/810AA; lanes 4 and 5) or abrogated (R837D and K882E; lanes 6 and 7; note that the charge differences caused R837D and K882E mutant proteins to migrate slower in the gel). Importantly, the Brat NHL R837D mutant can assemble into an NRE complex (see below; Figure 3, lane 4), demonstrating that this mutation specifically affects the d4EHP interaction and not the interactions with Pum and Nos.

Brat inhibits *hb* mRNA translation by interacting with the NRE complex [7]. Since d4EHP interacts physically with Brat, we asked whether d4EHP can be copurified with the NRE complex in vitro. Incubation of recombinant components of the NRE complex (Brat, Pum, Nos, and NRE) together with HA-tagged d4EHP resulted in the retention of d4EHP on glutathione-Sepharose beads through the GST-Pum RNAB fusion protein (Figure 3,

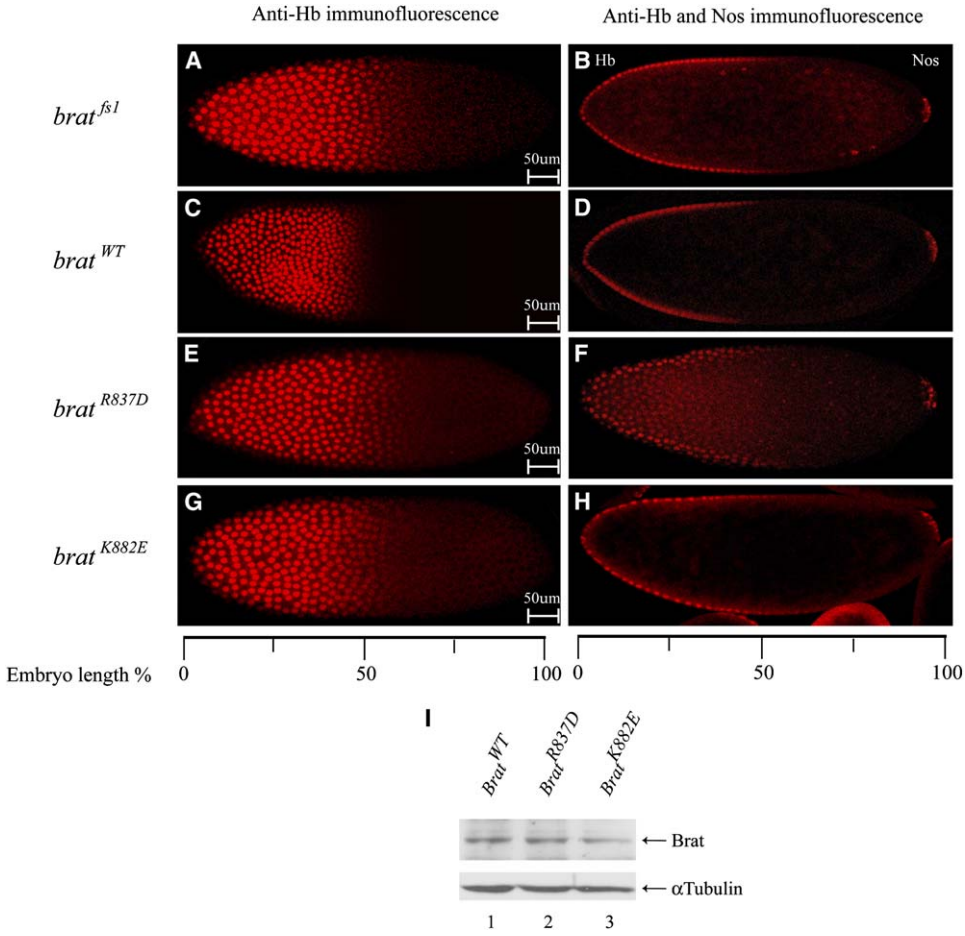

Figure 4. Functional Analysis of *brat* Mutants in Transgenic *Drosophila* Embryos

(A and B) Embryos derived from homozygous $brat^{fs1}$ females show a shift of the Hb expression boundary toward the posterior.
(C and D) Embryos derived from females expressing $brat^{WT}$ in the $brat^{fs1}$ mutant background show wild-type Hb distribution pattern.
(E–H) Embryos derived from females expressing mutant $brat^{R837D}$ and $brat^{K882E}$ genes (unable to bind d4EHP) exhibit ectopic Hb expression.
(B, D, F, and H) Embryos stained for both Hb and Nos proteins with the same secondary antibody, the latter serving as an internal control for staining intensity. The anterior tip is indicated as 0%. Orientation of embryos is anterior left and dorsal up.
(I) Western blot analysis of embryo extracts with anti-Brat or anti-α-tubulin as a loading control. Two to three independent transgenic lines were examined for each experiment, with similar results.

lane 2). The association of Brat with d4EHP was dependent on the ability of d4EHP to bind to Brat, since addition of Pum/Nos/NRE alone or in combination with the Brat R837D mutant failed to capture it (lanes 3 and 4). Thus, by interacting with Brat, d4EHP can associate with the NRE complex.

To investigate the biological significance of the d4EHP:Brat interaction, we studied the effects of Brat mutants, which are defective for d4EHP binding, in *Drosophila* embryos. As previously shown [7], $brat^{fs1}$ mutant embryos exhibit a significant expansion of the Hb expression domain toward the posterior (Figures 4A and 4B) and display severe abdominal segmentation defects (Table 1). When a $brat^{WT}$ transgene is expressed in the $brat^{fs1}$ mutant background, normal Hb distribution (Figures 4C and 4D) and a wild-type segmentation pattern is restored [7] (Table 1). To investigate whether interaction with d4EHP is essential for the function of Brat in embryonic patterning, we introduced transgenes encoding mutant forms of Brat that affect the d4EHP:Brat interaction ($brat^{R837D}$ and $brat^{K882E}$) into the $brat^{fs1}$ mutant background. Despite being expressed at levels similar to the $brat^{WT}$ transgene (Figure 4I), these mutant forms fail to fully rescue the normal Hb gradient (Figures 4E–4H) and, importantly, do not fully rescue the $brat^{fs1}$ mutant phenotype (Table 1). Taken together, our data strongly argue that the d4EHP:Brat interaction contributes significantly to *hb* regulation.

We have demonstrated here that through its interaction with Brat, d4EHP defines and sharpens the

Table 1. Abdominal Segmentation Defects in Brat Mutant Embryos

	Number of Abdominal Segments								
	0	1	2	3	4	5	6	7	8
$Brat^{fs1}/Df(2L)TE37C\text{-}7$	2	10	62	20	5	1			
$Brat^{fs1}/Df(2L)TE37C\text{-}7;\ Brat^{WT}$									100
$Brat^{fs1}/Df(2L)TE37C\text{-}7;\ Brat^{R837D}$						7	24	39	30
$Brat^{fs1}/Df(2L)TE37C\text{-}7;\ Brat^{K882E}$							20	41	39

Each entry is the percentage of embryos derived from females of the indicated genotype (left) bearing the indicated number of abdominal segments (above). 70 to 100 embryos were scored in each case.

posterior boundary of Hb expression. Based on the hypomorphic *d4EHP*^{CP53} phenotype, its activity appears most relevant to *hb* regulation in the region of the embryo from 50% to 75% EL, although it is possible that a null *d4EHP* allele would have more drastic effects. The d4EHP:Brat interaction is mediated via residues on the bottom surface of the Brat NHL domain (Figures 2F and 2G). Thus, as in the model we established for *cad* [10], a simultaneous interaction of d4EHP with the cap and Brat results in mRNA circularization and renders *hb* translationally inactive. Since the interaction between Brat and d4EHP does not involve the 4EHP binding motif we previously described (YxxxxxxLΦ), it is possible that d4EHP interacts with Brat through a bridging protein.

Our data support a model for the requirement for the 5′ cap structure in regulation of endogenous *hb* mRNA. This is consistent with an earlier study that assessed translation of NRE-containing mRNAs after injection into *Drosophila* embryos and concluded that the cap structure is functionally significant [9]. In contrast, another study reported that Nos and Pum repressed the expression of an engineered transgene containing an internal ribosome entry site (IRES) and a hairpin loop designed to block cap-dependent translation [23]. These results were used to conclude that *hb* translational repression is cap independent. However, the phenotypic assay used in that study was indirect and the observed results could also be caused by RNA destabilization. Furthermore, Nos-dependent deadenylation was also shown to be important in establishing the Hb gradient [20]. It is difficult to reconcile all these data without concluding that multiple distinct posttranscriptional mechanisms regulate Hb expression, including two that require Nos. The novel d4EHP-dependent mechanism we defined appears important for repressing *hb* in more central regions of the embryo, while cap-independent regulation involving deadenylation of *hb* mRNA may predominate in more posterior regions of the embryo. We note that mutant forms of Brat that are abrogated for d4EHP interaction retain substantial (but not complete) activity in repressing *hb*, suggesting some redundancy between these two mechanisms. Analogous overlapping translational control mechanisms have recently been reported for Bruno, which represses Oskar (Osk) expression both through cap-dependent translational regulation and through packaging *osk* mRNA into translationally silent RNP complexes [24].

Our identification of a common inhibitory mechanism that regulates *cad* and *hb* mRNA translation simplifies our understanding of how the anterior-posterior axis is organized during early *Drosophila* embryogenesis. By regulating two classical maternal morphogenetic gradients, d4EHP plays a critical role in early *Drosophila* embryonic development. It is noteworthy that d4EHP is recruited to these mRNAs through different RNA binding proteins that presumably recognize different sequence elements. In the case of *cad*, d4EHP becomes associated by binding directly to Bcd, which in turn recognizes a defined 3′UTR element, the BBR [25, 26]. In the case of *hb*, Bcd binding is not involved in d4EHP recruitment and no element similar to the BBR is present. It remains uncertain whether the interaction between d4EHP and Brat is direct or indirect; because d4EHP and Brat are both uniformly distributed in early embryos [7, 10], a non-uniformly distributed bridging protein mediating this interaction may be the basis of the spatially restricted requirement for d4EHP in *hb* repression. Since d4EHP and some of its interacting partners are evolutionarily conserved in higher eukaryotes and because cap-dependent translation regulation plays such an important role in eukaryotic gene expression [16], we predict that 4EHP-dependent translational inhibitory mechanisms are widespread throughout the animal kingdom.

Experimental Procedures

Plasmids

Cloning of *d4EHP* was previously described [10]. Brat cDNA (RE16276; Research Genetics) was obtained from the Berkeley *Drosophila* Genome Project [27]. All constructs reported herein were produced with the polymerase chain reaction (PCR). For *brat*, PCR-amplified wild-type and mutant cDNAs were introduced into the pcDNA3-N-term-FLAG vector via EcoRV/NotI sites. For recombinant protein expression, Brat NHL domain and Nos C-term domain (Nos C-term) were subcloned into the pProEx-His vector by means of SalI/NotI and EcoRI/XhoI sites, respectively, and Pum RNA binding domain (Pum RNAB) into the pGEX 6p-1 vector by means of EcoRI/SalI sites. NRE from *hb* mRNA, flanked by XbaI sites, was introduced into the 3′ UTR of pcDNA3-rLuc-ΔApaI reporter vector. To create pCaSpeR4-*nos* promoter-*Brat* wild-type and mutant rescue vectors, Brat constructs were inserted into the pKS-*nos* promoter vector by means of NheI/NotI sites. Subsequently, a Kpn1/NotI cassette from pKS-*nos* promoter-*Brat* wild-type and mutant vectors were transferred into the pCaSpeR4 vector. All inserts were fully sequenced.

Recombinant Protein Purification

E. coli BL21(DE3) transformed with the pProEx-Brat NHL domain, pProEx-Nos C-term, and pGEX-Pum RNAB constructs were used to produce His-Brat NHL domain, His-Nos C-term, and GST-Pum RNAB fusion proteins as previously described [10]. TALON Metal Affinity resin (BD Bioscience) and glutathione Sepharose 4B resin (Amersham Pharmacia) were used according to the manufacturers' instructions.

Brat Antibody and Western Blotting Analysis

A Brat antibody (#3187) was raised in a New Zealand White rabbit injected with recombinant His-Brat NHL domain protein and used for western blotting (1:3000). Cell culture, coimmunoprecipitation, and western blotting were performed as previously described [10].

Transgenic Rescue Experiment

Transgenic flies were generated by P element-mediated germline transformation of *yw* recipients with pCaSpeR-*nos* promoter-*Brat* wild-type and mutant rescue vectors. Transformed *brat* lines were crossed to the *brat*^{fs1} mutant and tested for the rescue of mutant phenotypes. pUASp-*d4EHP* transgenic lines [10] and antibody staining were performed as previously described [28]. Hb and Nos, Pum, and Brat immunostainings were visualized with Alexa Fluor 546 goat anti-rat IgG secondary and Alexa Fluor 488 goat anti-rabbit IgG secondary, respectively (1:500; Molecular Probes) with a confocal laser scanning microscope. Embryo images were analyzed for Hb gradient with Zeiss LSM data acquisition software.

In Vitro Transcription/Translation and Binding Assay

pcDNA3-3HA-d4EHP [10] and pcDNA3-rLuc-ΔApaI-NRE vectors were linearized with ApaI and transcribed with T7 RNA polymerase (MBI). Nuclease-treated rabbit reticulocyte lysate (Promega) was incubated for 1 hr at 30°C with 300 ng of HA-d4EHP mRNA. Subsequently, the extract was supplemented with components of the NRE complex, and the experiments of Figure 4 were performed as previously described [7, 29].

Image Analyses, Immunofluorescence Quantitation, and Data Analyses

0- to 2-hour-old embryos were immunostained with anti-Hb (1:10,000, a gift of P. Macdonald) and Alexa Fluor 546-conjugated

secondary antibodies (Molecular Probes), and DNA was stained with DAPI. Images were captured with a Zeiss LSM510 confocal microscope. Quantitation of the fluorescence intensity was performed with Openlab (Improvision) by recording the intensity values within a nucleus-sized area sliding along the anterior-posterior axis. Multiple embryos (6–16) for each genotype were measured at 38–50 positions along the anterior-posterior axis for a total of more than 3000 data points. For each embryo, length was normalized (0% = anterior pole, 100% = posterior pole), and measured intensities were normalized by subtracting the intensity recorded at the posterior pole and dividing this value by the maximum intensity measured within the same embryo. Individual data points could have values below zero if the local signal intensity was less than that at the posterior pole. To generate the average curve, the data points for each genotype were grouped in 38 bins (corresponding to the smallest sample set). For each bin, values were averaged and the resulting 38 points constitute the average curve.

Supplemental Data

Three Supplemental Figures can be found with this article online at http://www.current-biology.com/cgi/content/full/16/20/2035/DC1/.

Acknowledgments

We thank P. Macdonald (anti-Hb), N. Dostatny (pKS-*nos*-X-Bcd 3′UTR vector), and Z. Lev (*brat*^{fs1}) for reagents; J. Laliberte for confocal microscopy; Guillaume Lesage in the Cell Imaging and Analysis Network (CIAN) and Jelena Jevtic for valuable help with the image analyses and quantification; Y.R. Lee, H. Beili, B. Spelke, and C. Lister for technical assistance; and F. Poulin, M. Bidinosti, J. Chicoine, M. Ferraiuolo, B. Raught, A.-C. Gingras, L. Huck, K. Madjar, and other members of our labs for valuable discussions. Y.A.C.-P. was supported by the Canadian Institute of Health Research (CIHR) Burroughs Wellcome scholarship to medical students. N.S. is a CIHR Distinguished Scientist and a Howard Hughes Medical Institute (HHMI) International Scholar. This work was supported by grants from the CIHR to N.S. and P.L., by a grant from the NCIC with funds from the Canadian Cancer Society to P.L., and by a grant from the NIH (R01 GM66157) to N.S.

Received: May 22, 2006
Revised: August 18, 2006
Accepted: August 21, 2006
Published: October 23, 2006

References

1. Wickens, M., Goodwin, E.B., Kimble, J., Strickland, S., and Hentze, M. (2000). Translational control of developmental decision. In Translational Control of Gene Expression, N. Sonenberg, J.W.B. Hershey, and M.B. Mathews, eds. (Cold Spring Harbor, NY: Cold Spring Harbor Laboratory Press), pp. 295–370.
2. Gebauer, F., and Hentze, M.W. (2004). Molecular mechanisms of translational control. Nat. Rev. Mol. Cell Biol. *5*, 827–835.
3. St Johnston, D., and Nusslein-Volhard, C. (1992). The origin of pattern and polarity in the *Drosophila* embryo. Cell *68*, 201–219.
4. Johnstone, O., and Lasko, P. (2001). Translational regulation and RNA localization in *Drosophila* oocytes and embryos. Annu. Rev. Genet. *35*, 365–406.
5. Tautz, D., Lehmann, R., Schnürch, H., Schuh, R., Seifert, E., Kienlin, A., Jones, K., and Jäckle, H. (1987). Finger protein of novel structure encoded by *hunchback*, a second member of the gap class of *Drosophila* segmentation genes. Nature *327*, 383–389.
6. Tautz, D. (1988). Regulation of the *Drosophila* segmentation gene *hunchback* by two maternal morphogenetic centres. Nature *332*, 281–284.
7. Sonoda, J., and Wharton, R.P. (2001). *Drosophila* Brain Tumor is a translational repressor. Genes Dev. *15*, 762–773.
8. Wharton, R.P., and Struhl, G. (1991). RNA regulatory elements mediate control of *Drosophila* body pattern by the posterior morphogen nanos. Cell *67*, 955–967.
9. Chagnovich, D., and Lehmann, R. (2001). Poly(A)-independent regulation of maternal *hunchback* translation in the *Drosophila* embryo. Proc. Natl. Acad. Sci. USA *98*, 11359–11364.
10. Cho, P.F., Poulin, F., Cho-Park, Y.A., Cho-Park, I.B., Chicoine, J.B., Lasko, P., and Sonenberg, N. (2005). A new paradigm for translational control: inhibition via 5′-3′ mRNA tethering by Bicoid and the eIF4E cognate 4EHP. Cell *121*, 411–423.
11. Shatkin, A.J. (1976). Capping of eukaryotic mRNAs. Cell *9*, 645–653.
12. Hershey, J.W.B., and Merrick, W.C. (2000). Pathway and mechanism of initiation of protein synthesis. In Translational Control of Gene Expression, N. Sonenberg, J.W.B. Hershey, and M.B. Mathews, eds. (Cold Spring Harbor, NY: Cold Spring Harbor Laboratory Press), pp. 33–88.
13. Poulin, F., and Sonenberg, N. (2003). Mechanism of translation initiation in eukaryotes. In Translation Mechanisms, J. Lapointe and L. Brakier-Gingras, eds. (Austin, TX: Landes Bioscience), pp. 280–297.
14. Sachs, A. (2000). Physical and functional interactions between the mRNA cap structure and the poly(A) tail. In Translational Control of Gene Expression, N. Sonenberg, J.W.B. Hershey, and M.B. Mathews, eds. (Cold Spring Harbor, NY: Cold Spring Harbor Laboratory Press), pp. 447–466.
15. Kahvejian, A., Svitkin, Y.V., Sukarieh, R., M'Boutchou, M.N., and Sonenberg, N. (2005). Mammalian poly(A)-binding protein is a eukaryotic translation initiation factor, which acts via multiple mechanisms. Genes Dev. *19*, 104–113.
16. Richter, J.D., and Sonenberg, N. (2005). Regulation of cap-dependent translation by eIF4E inhibitory proteins. Nature *433*, 477–480.
17. Khaleghpour, K., Svitkin, Y.V., Craig, A.W., DeMaria, C.T., Deo, R.C., Burley, S.K., and Sonenberg, N. (2001). Translational repression by a novel partner of human poly(A) binding protein, Paip2. Mol. Cell *7*, 205–216.
18. Struhl, G., Johnston, P., and Lawrence, P.A. (1992). Control of *Drosophila* body pattern by the hunchback morphogen gradient. Cell *69*, 237–249.
19. Lehmann, R., and Nusslein-Volhard, C. (1987). *hunchback*, a gene required for segmentation of an anterior and posterior region of the *Drosophila* embryo. Dev. Biol. *119*, 402–417.
20. Wreden, C., Verrotti, A.C., Schisa, J.A., Lieberfarb, M.E., and Strickland, S. (1997). Nanos and Pumilio establish embryonic polarity in *Drosophila* by promoting posterior deadenylation of *hunchback* mRNA. Development *124*, 3015–3023.
21. Marcotrigiano, J., Gingras, A.-C., Sonenberg, N., and Burley, S.K. (1997). Cocrystal structure of the messenger RNA 5′ cap-binding protein (eIF4E) bound to 7-methyl-GDP. Cell *89*, 951–961.
22. Edwards, T.A., Wilkinson, B.D., Wharton, R.P., and Aggarwal, A.K. (2003). Model of the Brain Tumor-Pumilio translation repressor complex. Genes Dev. *17*, 2508–2513.
23. Wharton, R.P., Sonoda, J., Lee, T., Patterson, M., and Murata, Y. (1998). The Pumilio RNA-binding domain is also a translational regulator. Mol. Cell *1*, 863–872.
24. Chekulaeva, M., Hentze, M.W., and Ephrussi, A. (2006). Bruno acts as a dual repressor of *oskar* translation, promoting mRNA oligomerization and formation of silencing particles. Cell *124*, 521–533.
25. Dubnau, J., and Struhl, G. (1996). RNA recognition and translational regulation by a homeodomain protein. Nature *379*, 694–699.
26. Rivera-Pomar, R., Niessing, D., Schmidt-Ott, U., Gehring, W.J., and Jäckle, H. (1996). RNA binding and translational suppression by Bicoid. Nature *379*, 746–749.
27. Rubin, G.M., Hong, L., Brokstein, P., Evans-Holm, M., Frise, E., Stapleton, M., and Harvey, D.A. (2000). A *Drosophila* complementary DNA resource. Science *287*, 2222–2224.
28. Kobayashi, S., Amikura, R., Nakamura, A., and Lasko, P.F. (1999). Techniques for analyzing protein and RNA distribution in *Drosophila* ovaries and embryos at structural and ultrastructural resolution. In Advances in Molecular Biology: A Comparative Methods Approach to the Study of Oocytes and Embryos, J. Richter, ed. (New York: Oxford University Press), pp. 426–445.
29. Sonoda, J., and Wharton, R.P. (1999). Recruitment of Nanos to *hunchback* mRNA by Pumilio. Genes Dev. *13*, 2704–2712.